

## Parameterizing the Height of the Stable Atmospheric Boundary Layer

S. P. S. ARYA

*Department of Marine, Earth and Atmospheric Sciences, North Carolina State University, Raleigh, 27650*

(Manuscript received 30 July 1980, in final form 23 June 1981)

### ABSTRACT

A critical assessment is made of the various diagnostic relations for the height of the nocturnal boundary layer, as well as of their past comparisons with experimental data. The parametric relations involving the characteristics of the whole boundary layer are found to be less satisfactory than those involving only the surface layer variables. The latter are tested against the Cabauw tower data for the selected winter periods when the mixed-layer height  $h$  was measured directly with an acoustic sounder. It is found that  $h$  has rather poor correlation with the height  $h_0$  to which the effect of surface cooling extends. Its correlation with  $h_u$ , the height of the maximum in wind speed, is fair ( $r \approx 0.5$ ) during strong stability conditions, but poor in slight to moderate stability conditions. Better correlations ( $r \approx 0.7$ ) are obtained with  $u_* f$ ,  $(u_* L f)^{1/2}$  and Deardorff's (1972b) interpolation formula where  $u_*$  is the friction velocity,  $L$  is the Obukhov length and  $f$  the Coriolis parameter. The parametric relations based on the linear regression of  $h$  with the above height parameters are given. These may be used in the absence of direct measurements of  $h$ , especially when the type of information required for using a more accurate prognostic rate equation is not available.

### 1. Introduction

The height  $h$  of the atmospheric boundary layer (ABL) may, in general, be defined as the height to which insignificant turbulent transfers of heat, mass and momentum between the local earth's surface and the atmosphere occur when averaged over a period of the order of an hour. It is probably the most important parameter influencing its mean flow and turbulence structure. Dimensions of the largest eddies, including roll vortices, over a flat and homogeneous terrain are essentially fixed by  $h$ . Wind shears, turbulence intensities and fluxes in the ABL also strongly depend on  $h$ . It is not surprising that the most generalized similarity theory formulations consider the ABL height as an independent parameter which appears in almost all of the dimensionless similarity parameters (Deardorff, 1972a; Zilitinkevich and Deardorff, 1974; Arya and Sundararajan, 1976). The height of the ABL is also required to be specified or parameterized in several generalized schemes for parameterizing the boundary layer in large-scale atmospheric circulation models (Deardorff, 1972b; Arya, 1975, 1977). It is also, of course, an important parameter in modeling and predicting atmospheric dispersion from a variety of pollutant sources within the ABL. In air pollution meteorology,  $h$  is more commonly known as the mixing depth.

The daytime unstable or convective ABL is

usually capped by an inversion and  $h$  approximately coincides with the height of the inversion base for which a number of simple and reliable methods of measurement, as well as dependable prognostic models of computation are available. For the nighttime stable boundary layer, however, both the measurement and prediction of  $h$  have proven to be far more difficult and less reliable. An upward looking sodar (acoustic sounder) and a lidar provide the only reliable means of measuring the height of the shallow and weakly mixed boundary layer that commonly occurs during nighttime stable conditions over land. When such direct measurements of  $h$  are not available, as often is the case for most routine meteorological observations, the height of the stable boundary layer is estimated through the use of certain parametric relations between  $h$  and other boundary-layer parameters that have been proposed in the literature. Such relations are often based on simple intuitive and theoretical considerations and have rarely been tested against direct measurements of  $h$ , although indirect estimates have been used for such testing purposes (Hanna, 1969; Yu, 1978). The main objective of this note is to make a comparative assessment of some of the better known parameterizations of the height of the nocturnal ABL on the basis of its direct measurement by an acoustic sounder and simultaneous micro-meteorological measurements from the 213 and 20 m masts at Cabauw in the Netherlands.

## 2. Parametric relations for $h$

### a. Relationship with other characteristic heights

In the absence of any direct measurements of the height of the stably stratified ABL,  $h$  has often been identified with the following characteristic heights, which can be determined from the observed velocity and temperature profiles:

1)  $h_e$ , the Ekman height at which the mean wind vector first becomes parallel to the geostrophic wind (Taylor, 1915). This height can be determined unambiguously only from theoretical wind spirals. It is difficult to determine from the observed wind hodograph because of the large experimental errors in estimating geostrophic winds and their variation with height.

2)  $h_u$ , the height of maximum in wind speed profile or the so-called low-level jet (Blackadar, 1957). This height is generally well defined from the nighttime wind profiles over land.

3)  $h_i$ , the height of the nocturnal surface inversion, the top of which can be defined as the lowest level where the temperature gradient exhibits a discontinuity or reduces approximately to its dry adiabatic value. This height cannot be well defined when potential temperature increases monotonically to large heights.

4)  $h_\theta$ , the height to which a significant cooling extends, as judged from the evolution of the potential temperature profile in time (Melgarejo and Deardorff, 1974).

### b. Diagnostic relations

Steady-state models of nocturnal boundary layers have led to a number of diagnostic height relations, which can be broadly divided into two groups. The first group involves the characteristics of the whole boundary layer, such as the magnitude of the surface geostrophic wind  $G_0$ , the layer-averaged vertical potential temperature gradient  $\langle \partial\bar{\theta}/\partial z \rangle$ , etc. For example, earlier models of Rossby and Montgomery (1935) and Laikhtman (1961) have given the relation

$$h = cG_0 \left( \frac{g}{T_0} \left\langle \frac{\partial\bar{\theta}}{\partial z} \right\rangle \right)^{-1/2}, \quad (1)$$

in which  $g/T_0$  is the buoyancy parameter and  $c$  is a constant. The relations of this type imply or assume that the bulk Richardson number or the Froude number based on the boundary-layer height is a constant for all stable boundary layers, i.e., the boundary layer adjusts its height until this criterion is met.

The second group of diagnostic relations involve only the surface-layer variables, such as the friction velocity  $u_*$  and Obukhov length  $L$ . Various contemporary numerical models (Businger and Arya,

1974; Wyngaard, 1975; Brost and Wyngaard, 1978; Rao and Snodgrass, 1979) of the nocturnal ABL have confirmed the relation, first suggested by Zilitinkevich (1972),

$$h = d \left( L \frac{u_*}{f} \right)^{1/2}, \quad (2)$$

in which  $d$  is a constant of the order one (the exact value appears to be quite sensitive to model assumptions).

Some investigators (Benkley and Schulman, 1979) have suggested that for routine operational use, the simpler relation

$$h = a \frac{u_*}{f}, \quad (3)$$

which is valid for the neutral case, might also be used for the nocturnal boundary layer. The constant  $a$  may be expected to be somewhat smaller than its neutral value of  $\sim 0.3$ . An alternative relationship

$$h = bL \quad (4)$$

is considered to be more appropriate for strongly stratified conditions encountered at nighttime. The constant  $b$  is of the order of 10, whose exact value still remains to be determined.

### c. Prognostic relations

The diagnostic formulas discussed in the previous section are strictly valid for steady state conditions. Similar to the daytime unstable boundary layer over land, the nocturnal ABL in reality has been observed to display transient or evolutionary characteristics, though the variations in  $h$  are not as pronounced as under convective conditions. In particular, the height of surface inversion  $h_i$  has been found to grow from a value of  $< 100$  m shortly after sunset to a height typically 200–500 m by early next morning. This tendency of  $h_i$  to increase, in spite of increasing stability, may only reflect the tendency of a nocturnal jet to develop near the top of the stable ABL (Zilitinkevich and Deardorff, 1974). It is not clear whether a prognostic rate equation for  $h_i$  would be appropriate under these conditions. However, Yamada (1979) and Nieuwstadt (1980) have derived equations for the evolution of the nocturnal surface inversion height, using the mean thermodynamic energy equation with rather crude parameterizations for the radiative flux-divergence term.

Prognostic rate equations for the nocturnal mixing depth  $h$  have also been proposed (Zilitinkevich and Monin, 1974; Zeman, 1979; Smeda, 1979; Nieuwstadt and Tennekes, 1981). For example, using the integral forms of the equations of mean momentum, thermodynamic energy and turbulent kinetic energy,

together with certain plausible similarity relations, Nieuwstadt and Tennekes (1981) have derived a linear relaxation-type rate equation

$$\frac{dh}{dt} = \frac{h_e - h}{t_s}, \quad (5)$$

where  $h_e$  is the equilibrium value of  $h$  and  $t_s = -0.75 \times (\theta_n - \theta_0)(d\bar{\theta}_0/dt)^{-1}$  is a time scale characterizing the rate at which the solution is forced toward the equilibrium height. Since,  $t_s$  is a monotonically increasing function of time (varying from a few hours during early night to an order of 10 h early next morning), boundary-layer height according to Eq. (5) evolves at a decreasing rate, never quite reaching its equilibrium height  $h_e$ , which is given by a diagnostic relation of the type (1) discussed earlier. This predicted slow approach to steady-state equilibrium height has prompted some investigators to question the validity and usefulness of diagnostic relations for estimating the nocturnal boundary-layer height (Nieuwstadt, 1981).

There is no doubt that a good prognostic model of  $h$  incorporating the essential physics of the evolutionary processes in the nocturnal ABL should do better than the best of diagnostic relations based on the questionable assumptions of steady state and equilibrium during nighttime conditions. Therefore, the former must be used whenever possible, i.e., when the required information is available. Unfortunately, however, in many practical situations, the required information, such as the value of  $h$  at some initial time  $t_0$  after the evening transition and the potential temperature  $\bar{\theta}_n$  at  $z = h$ , may not be available. In such cases, the diagnostic height relations may provide the only means of estimating  $h$ . With this in view, we examine here the relative utility of the various diagnostic height formulas on the basis of their comparisons with observations.

### 3. Past comparisons with experimental data

A comparative evaluation and testing of some of the proposed diagnostic relations discussed in the previous section was done by Hanna (1969) using the data taken during the Great Plains Experiment at O'Neil, Nebraska (Lettau and Davidson, 1957). Since direct measurements of the mixing depth  $h$  were not made, Hanna used  $h_i$  (defined as the lowest level at which the temperature lapse rate exhibited a discontinuity) as a measure of the ABL height. This he plotted and correlated against the characteristic heights  $h_e$  and  $h_u$  based on velocity profiles,  $G_0 f$ ,  $u_* f$ ,  $G_0 [(g/T_0)(\partial\bar{\theta}/\partial z)]^{-1/2}$  and  $G_0 \sin\alpha_0 [(g/T_0) \times (\partial\bar{\theta}/\partial z)]^{-1/2}$ . Unfortunately, observations were not separated according to stability, so that stable and unstable data appear to be all mixed. One can, however, roughly separate out the data corresponding to nocturnal stable conditions as those with  $h_i \leq 500$  m. With this criterion, according to the graphs

presented by Hanna (1969),  $h_i$  has no significant correlation with  $h_e$ , fair correlation with  $h_u$ , rather poor correlation with  $G_0 f$  and  $u_* f$ , and good correlation (correlation coefficient  $r \approx 0.89$ ) with  $G_0 [(g/T_0)(\partial\bar{\theta}/\partial z)]^{-1/2}$ . On the basis of this study, Hanna concluded that Laikhtman's (1961) formula (1) with his revised value of  $c = 0.75$  for the coefficient is the best formula for estimating the boundary-layer height, but it is not very practical because it is difficult to estimate  $\langle \partial\bar{\theta}/\partial z \rangle$  without the use of a tall meteorological tower or radiosonde equipment. One can, however, argue that if temperature soundings are available,  $h_i$  can be estimated directly from the same and there is no need of employing an uncertain empirical formula. Aside from its practical utility, is Laikhtman's formula as good as Hanna has shown it to be?

In order to answer the above question, one should carefully examine the possibility of an inadvertent spurious correlation introduced in the data by Hanna's analysis procedure. Since he used the approximation

$$\left\langle \frac{\partial\bar{\theta}}{\partial z} \right\rangle \approx \frac{\bar{\theta}(h_i) - \bar{\theta}(100 \text{ m})}{h_i - 100 \text{ m}}, \quad (6a)$$

it is very likely that a significant spurious correlation got introduced due to the appearance of  $h_i$  in the correlated variable. This is probably the reason why the same relation for  $h_i$  was also found to be valid for the daytime unstable conditions in which one would not really expect such a simple relationship to hold.

Alternatively, if one uses an approximate, but plausible, relation

$$\left\langle \frac{\partial\bar{\theta}}{\partial z} \right\rangle \propto \frac{\Delta\bar{\theta}}{h_i}, \quad (6b)$$

which is not much different from (6a), its substitution in Laikhtman's formula yields

$$h_i = CG_0^2 \left( \frac{g}{T_0} \Delta\bar{\theta} \right)^{-1}, \quad (7)$$

where  $C$  is a constant of the order of unity. Note that Eq. (7) or the similar relation suggested by Pollard *et al.* (1973), from a practical point of view, is a more useful parametric relation for  $h_i$  than Laikhtman's formula, because it requires the knowledge of the bulk temperature difference across the boundary layer rather than the detailed vertical profile for estimating the layer-averaged gradient  $\langle \partial\bar{\theta}/\partial z \rangle$ . Eq. (7) also can be tested against experimental data without the risk of introducing any spurious correlation. As pointed out earlier, however, Eq. (7) and other diagnostic formulas of this type imply a constant value of the bulk Richardson number or Froude number for all stable conditions. It is doubtful that such a simple state of affairs actually exists. The bulk Richardson number is

expected to increase with increasing stability and may approach a constant value only under extremely stable conditions (Deardorff, 1972b). This is confirmed by the wide range of the bulk Richardson number values obtained from both the O'Neil and Wangara data (Arya, 1975).

Wyngaard (1975) presented some measurements of  $h$  (defined as the height where turbulent heat flux vanishes) as a function of time during one night of the 1973 Minnesota experiment and showed that they agreed well with his numerical model simulation. Recently, Caughey *et al.* (1979) have shown that the Minnesota observations of the nocturnal ABL height are consistent with Eq. (2) with  $d \approx 0.7$ , although these observations do not represent steady-state conditions. Since observations of only one night were used in their comparison, the above estimate of the constant  $d$  may not be very accurate. In fact, second-order-closure model simulations of Brost and Wyngaard (1978) indicate that  $d$  is a decreasing function of the time after transition, attaining a constant value of about 0.4 only after 6 h. The value of  $d$  is also dependent on such factors as the rate of cooling, drainage and thermal winds, etc.

In another comparison, Arya (1977) used the extensive three-hourly observations from the Wangara experiment. In the absence of direct measurements of  $h$ , the values of surface inversion height  $h_i$  were plotted against the corresponding values of  $(Lu_*f)^{1/2}$  obtained from the surface layer data. The correlation between the two was found to be only marginally significant ( $r \approx 0.43$ ). The observed values of  $h_i$  ranged between 100 and 600 m, irrespective of the stability classification based on  $L$  values. A similar scatter diagram resulted when the observed surface inversion heights were compared with Deardorff's (1972b) interpolation formula

$$h = \left( \frac{1}{30L} + \frac{f}{0.35u_*} \right)^{-1}. \quad (8)$$

Yu (1978) also used the Wangara data to test some of the proposed diagnostic and prognostic relations for the nocturnal boundary-layer height. He used the characteristic heights  $h_u$ ,  $h_i$  and  $h_\theta$  as different measure of  $h$ . The correlation coefficients ( $r$  values) between the observed values of  $h_u$  and  $h_\theta$  and the scale heights  $ku_*f$ ,  $(kLu_*f)^{1/2}$  and  $[(1/30L) + (f/0.35u_*)]^{-1}$  ranged between 0.42 and 0.46, considering all the 60 runs irrespective of the stability class. When separated according to stability classes based on  $\mu_* \equiv u_*fL$ , the  $r$  values are seen to be considerably larger ( $r > 0.7$ ) for the slightly stable category ( $5 < \mu_* < 27$ ), reduce to nearly zero for the very stable ( $45 < \mu_* < 78$ ), class and increase again for the extremely stable ( $\mu_* > 78$ ) category. Both  $h_u$  and  $h_\theta$  correlate equally well with the diagnostic formulas, while  $h_i$  exhibits the least correlation ( $r < 0.25$ ). However, Yu did

not calculate the coefficients of linear regression between the observed heights and the diagnostic height parameters; his paper implied the use of the parametric relations

$$\left. \begin{aligned} h_u \approx h_\theta \approx ku_*f \\ h_u \approx h_\theta \approx (ku_*L/f)^{1/2} \\ \text{etc.} \end{aligned} \right\}. \quad (9)$$

Mahrt and Heald (1979), in a comment on Yu's (1978) paper, have pointed out that the reason for similar correlations between the various observed heights and  $ku_*f$ ,  $(ku_*L/f)^{1/2}$ , etc., is the very high correlation ( $r = 0.92$ ) between  $u_*$  and  $L$ . They also showed that the observed characteristic heights  $h_u$ ,  $h_\theta$  and  $h_i$  are poorly correlated with each other [ $r(h_\theta, h_u) \approx 0.20$ ,  $r(h_i, h_u) \approx 0.19$ ,  $r(h_i, h_\theta) \approx 0.58$ ]. This again points out the need of using direct observations of the mixing depth for testing the various height formulas.

More recently, Mahrt *et al.* (1979) have examined the mean structure of the nocturnal boundary layer on the basis of the earlier O'Neil and the Wangara observations, as well as more recent aircraft and acoustic sounder observations at Haswell, Colorado. They find that, on the average, the top of the boundary layer occurs just below the low-level wind maximum, which, in turn, approximately coincides with the height of the maximum in gradient Richardson number. However,  $h_i$  is often  $\sim 25\%$  higher than  $h_u$  due to clear-air radiational cooling;  $h_u$  is probably a better measure of  $h$ , especially in strongly stratified conditions with a well developed low-level jet.

Nieuwstadt and Driedonks (1979) used measurements of  $h$  (by acoustic sounder) and turbulent fluxes of momentum and heat at the 213 m Cabauw mast, during one-night period, to show that Eq. (2) may be a poor predictor for the nocturnal boundary-layer height. More recently, Nieuwstadt (1981) arrived at the same conclusion from an analysis of more extensive Cabauw (1975) data. It appears that under strong stability conditions, boundary layer does not attain steady state and its height may not be determined in terms of local parameters. The prognostic relation (5) describing the evolution of  $h$  is found to be more satisfactory (Nieuwstadt and Tennekes, 1981).

In this study, we have used a part of the same (Cabauw, 1975) data to further test the validity of diagnostic relations for the nocturnal boundary-layer height. Our analysis differs from Nieuwstadt's mainly in the use of calculated  $u_*$  and  $L$  from the low-level ( $z < 10$  m) mean velocity and temperature measurements.

#### 4. Cabauw observations and their analysis

The data used here for testing the various diagnostic height relations were taken in February 1975

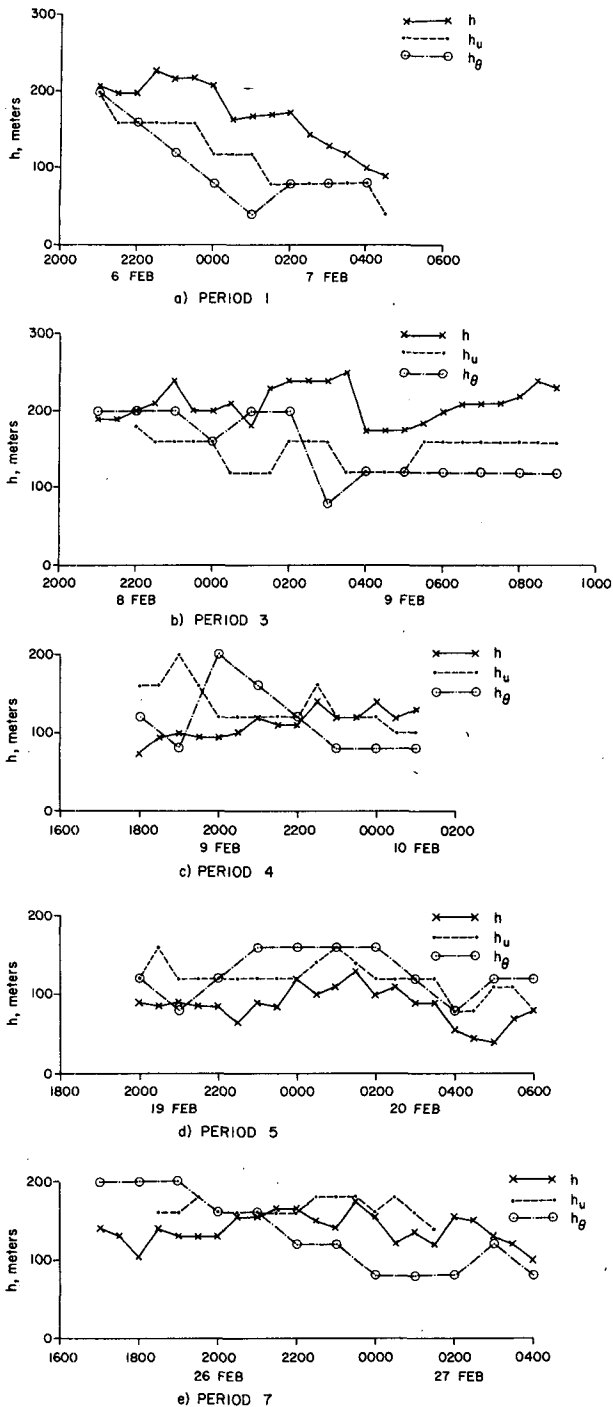


FIG. 1. Comparison of the sodar measured mixed-layer height ( $h$ ) with other characteristic heights of the nocturnal boundary layer during different observation periods at Cabauw.

by the Royal Netherlands Meteorological Institute near Cabauw, the Netherlands. A detailed description of the terrain, micrometeorological masts and instrumentation is given elsewhere.<sup>1,2</sup> The surround-

ings are topographically flat within a radius of 20 km in all directions, but are not uniform in their roughness characteristics. The immediate surroundings of the masts consist of meadows, but there are occasional lines of trees, river dikes, orchards and houses in the area.

The facilities included an instrumented 213 m high mast, two 20 m masts and an acoustic sounder or sodar for measuring the thermal structure up to 1000 m. Instruments for measuring temperature, wind speed and wind direction were located at 20 m intervals on the tower with additional measurements levels near the surface. In this analysis, we have used half-hourly averages of wind speed and temperature for selected periods of February, 1975. Half-hour averages of the mixed-layer height  $h$  were obtained from the continuous acoustic sounder returns. Only those periods were selected during which the top of the boundary layer as seen from the sodar returns was unambiguously demarcated. The characteristic heights  $h_u$  and  $h_\theta$  were determined from the observed mean wind speed and potential temperature profiles, which are more representative of the mean structure than the conventional radiosonde and pilot-balloon soundings. Due to the limited height of the tower, however,  $h_i$  could not be determined; it probably exceeded the tower height on most of the occasions.

A comparison of the sodar-measured  $h$  with other characteristic heights  $h_u$  and  $h_\theta$  is made in Fig. 1 for the selected observation periods in which all three could be determined. It clearly shows that, in general, neither  $h_u$  nor  $h_\theta$  can be considered identical to the mixed layer height  $h$ . On a number of occasions, however,  $h_u$  lies fairly close to  $h$  (see, e.g., the last parts of the periods 4, 5, and 7). During the other periods shown in Fig. 1,  $h_u$  is considerably smaller than  $h$ , implying that the wind maximum occurred somewhere in the middle of the mixed layer rather than near its top. It also appears that  $h_\theta$  might be a poorer measure of  $h$  than  $h_u$  is. A more objective comparison including correlation coefficients between  $h$  vs  $h_u$  and  $h$  vs  $h_\theta$  will be made later.

#### a. Computation of $u_*$ and $L$

The lowest measurement level (2 m) on the tower is well within the surface layer, even at night time. The next level at 9 m for temperature or 10 m for velocity measurements is likely to fall outside the nocturnal surface layer, especially during strongly stratified conditions. This point had to be con-

at Cabauw in 1973. Roy. Neth. Meteor. Inst., Sci. Rep. 76-7, 17 pp.

<sup>2</sup> Driedonks, A. G. M., H. van Dop and W. H. Kolsiek, 1978: Meteorological observations on the 213 m mast at Cabauw, in the Netherlands. *Preprints Fourth Symposium on Meteorological Observation and Instrumentation*, Denver, Amer. Meteor. Soc., 41-46.

<sup>1</sup> van Ulden, A. P., J. G. van der Vliet, and J. Wieringa, 1976: Temperature and wind observations at heights from 2 m to 200 m

sidered in calculating  $u_*$  and  $L$  from the available measurements at the above two levels. For the sake of convenience, the observed wind speeds at the 10 m level were used to obtain the estimated values for the 9 m level, at which temperature was measured, through the use of an approximate relationship based on the logarithmic wind profile

$$\bar{u}(9\text{ m}) = \left[ \frac{\ln 9 - \ln z_0}{\ln 10 - \ln z_0} \right] \bar{u}(10\text{ m}), \quad (10)$$

which may be justified because of the small (10%) difference between the above two levels. Here  $z_0$  is the surface roughness parameter in meters, which was determined from 13 near-neutral wind profiles, each averaged over a period of 2–3 h. Using the wind observations at 2, 10 and 40 m heights, we have estimated a geometric mean value of  $z_0 \approx 0.025$  m for the wind directions from northeast to east, and  $z_0 \approx 0.006$  m for the other wind directions. These values appear to be reasonable for the smoother terrain (flat meadow with 0.10 m high grass) immediately surrounding the mast, but are an order of magnitude less than the  $z_0$  values quoted by Driedonks *et al.* (1978) and Nieuwstadt (1978). Their large values ( $z_0 \approx 0.05 - 0.35$  m) are presumably more representative of the rougher terrain farther upwind that influences the planetary boundary layer as a whole, and not so representative of the local terrain influencing the surface layer. Because of these terrain inhomogeneities, it is doubtful that an equilibrium constant flux layer of more than a few meters in thickness would have existed at the mast site. Only the local surface shear stress at the site of smaller mast may be calculated from wind and temperature observations at the lowest (2 m) level, using the surface-layer similarity theory. This would be expected to be less than the average shear stress over a larger area incorporating lines of trees, orchards, houses, etc. In the absence of any direct estimates of the later, the local friction velocity  $u_*$  and  $L$  will be used for determining the various diagnostic heights and the stability parameter  $\mu_*$ .

The method used to compute local  $u_*$  and  $L$  is based on the assumption that the velocity profile is log-linear up to the first observation level so that

$$\bar{u}_1 = \frac{u_*}{k} \left[ \ln \frac{z_1}{z_0} + \beta \frac{z_1}{L} \right], \quad (11)$$

where  $\bar{u}_1$  is the velocity at the height  $z_1 = 2$  m and constants  $k \approx 0.35$  and  $\beta \approx 4.7$  are based on the study by Businger *et al.* (1971). Further assumption about the equality of the eddy diffusivities of heat and momentum up to the second observation level ( $z_2 = 9$  m) gives the following simple expression for the ratio of the vertical momentum and heat fluxes:

$$\frac{\overline{u'w'}}{\overline{\theta'w'}} = \frac{\partial \bar{u} / \partial z}{\partial \bar{\theta} / \partial z}. \quad (12)$$

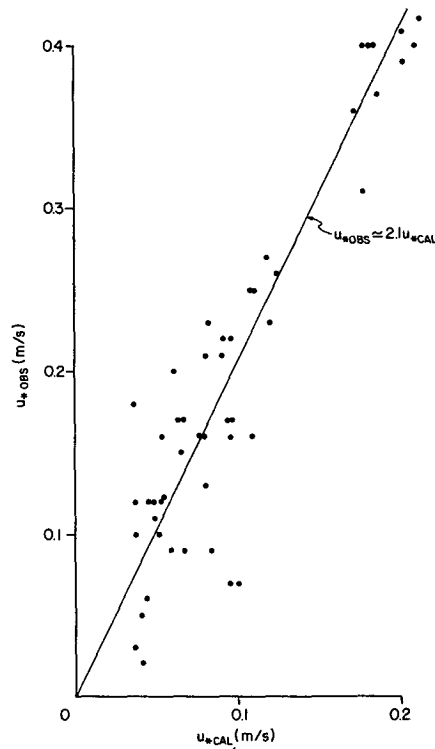


FIG. 2. Comparison of the observed  $u_*$  from eddy correlation flux measurements at 20 m with the computed  $u_*$  for the near-surface layer.

It may also be reasonable to assume that in the lower part ( $z \leq z_2$ ) of the nocturnal boundary layer, the momentum and heat flux profiles have similar shapes (Wyngaard, 1975; Caughey *et al.*, 1979). With this assumption, integration of Eq. (12) with respect to  $z$  from  $z_1$  to  $z_2$  yields

$$\frac{u_*}{\theta_*} = \frac{\Delta \bar{u}}{\Delta \bar{\theta}}, \quad (13)$$

where  $u_* = (-\overline{u'w'})_0^{1/2}$  and  $\theta_* = -(\overline{w'\theta'})_0/u_*$  are the friction velocity and temperature scales, and  $\Delta \bar{u} = \bar{u}_2 - \bar{u}_1$ , and  $\Delta \bar{\theta} = \bar{\theta}_2 - \bar{\theta}_1$  are the difference in velocity and potential temperature between the two heights. Eqs. (11) and (13) yield the expressions

$$\left. \begin{aligned} u_* &= \frac{k\bar{u}_1 - k\beta \frac{g}{T_0} \frac{\Delta \bar{\theta}}{\Delta \bar{u}} z_1}{\ln(z_1/z_0)} \\ L &= u_* \left( k \frac{g}{T_0} \frac{\Delta \bar{\theta}}{\Delta \bar{u}} \right)^{-1} \end{aligned} \right\}, \quad (14)$$

which have been used for calculating  $u_*$  and  $L$  from the observed values of  $\bar{u}_1$ ,  $\Delta \bar{u}$  and  $\Delta \bar{\theta}$ .

During parts of the observation periods considered here, eddy correlation measurements of momentum and heat fluxes also were made at the height of 20 m (Nieuwstadt, private communication). The "observed"  $u_* = (-\overline{u'w'})^{1/2}$  and  $L = (-\overline{u'w'})^{3/2}$

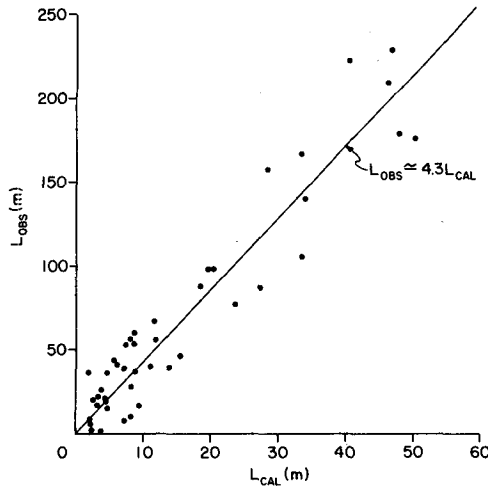


FIG. 3. Comparison of the observed  $L$  from eddy correlation flux measurements at 20 m with the computed  $L$  for the near-surface layer.

$[k(g/T_0)\overline{w'\theta'}]$  at 20 m are compared with our computed values of  $u_*$  and  $L$  for the near surface layer in Figs. 2 and 3. Although there is a good correlation between the observed and computed values, the

observed  $u_*$  at 20 m is on the average about twice the local surface value of  $u_*$ , and the observed  $L$  at 20 m is nearly four times the computed near-surface value of  $L$ . These comparisons indicate the existence of a strong positive gradient of momentum flux within the lowest 20 m layer. It is also likely that our assumption about the applicability of the surface-layer similarity theory to the lowest layer at Cabauw mast site may not be completely justified. In the following, the computed  $u_*$  and  $L$  from low-level wind and temperature measurements are used to test the diagnostic height relations, because such measurements are more likely to be available in routine applications of PBL height relations.

*b. Computed correlation and regression coefficients*

In addition to the half-hourly observations during the five periods represented in Fig. 1, we also used those for the nights of 7–8 February (period 2) and 25–26 February (period 6). Due to comparatively weak stratification occurring during these two periods, however, value of  $h_0$  could not be determined. For the period 6,  $h_u$  was also not determined, because well defined maximum did not occur within the tower layer. From a total of 151

TABLE 1. Correlation coefficients ( $r$  values) between the observed PBL height ( $h$ ) and the diagnostic height parameters.

| Stability class   | Diagnostic height parameter correlated with $h$ |        |        |                 |                                     |   |
|---|---|--------|--------|-----------------|-------------------------------------|---|
|   | $h_0$   | $h_u$  | $L$    | $\frac{u_*}{f}$ | $\left(\frac{Lu_*}{f}\right)^{1/2}$ | $\left(\frac{1}{30L} + \frac{f}{0.35u_*}\right)^{-1}$ |
| <b>Moderately stable</b><br>( $10 \leq \mu_* \leq 50$ )           |   |        |        |                 |                                     |   |
| $r$   | 0.53  | -0.09* | 0.41   | 0.31            | 0.41                                | 0.38  |
| $P$   | (0.02)  | (0.68) | (0.01) | (0.05)          | (0.01)                              | (0.01)  |
| $N$   | 18  | 24     | 41     | 41              | 41                                  | 41  |
| <b>Very stable</b><br>( $50 < \mu_* \leq 100$ )                   |   |        |        |                 |                                     |   |
| $r$   | 0.40  | 0.54   | 0.41   | 0.28*           | 0.36                                | 0.35  |
| $P$   | (0.01)  | (0.00) | (0.01) | (0.06)          | (0.01)                              | (0.02)  |
| $N$   | 44  | 37     | 44     | 44              | 44                                  | 44  |
| <b>Extremely stable</b><br>( $\mu_* > 100$ )                      |   |        |        |                 |                                     |   |
| $r$   | -0.23*  | 0.33*  | 0.11*  | 0.09*           | 0.10*                               | 0.11*   |
| $P$   | (0.26)  | (0.10) | (0.60) | (0.67)          | (0.62)                              | (0.60)  |
| $N$   | 26  | 25     | 26     | 26              | 26                                  | 26  |
| <b>Moderately and very stable</b><br>( $10 \leq \mu_* \leq 100$ ) |   |        |        |                 |                                     |   |
| $r$   | 0.45  | 0.07*  | 0.58   | 0.56            | 0.61                                | 0.61  |
| $P$   | (0.00)  | (0.58) | (0.00) | (0.00)          | (0.00)                              | (0.00)  |
| $N$   | 62  | 61     | 85     | 85              | 85                                  | 85  |
| <b>All stable cases with <math>\mu_* \geq 10</math></b>           |   |        |        |                 |                                     |   |
| $r$   | 0.28  | 0.10*  | 0.63   | 0.63            | 0.67                                | 0.67  |
| $P$   | (0.01)  | (0.37) | (0.00) | (0.00)          | (0.00)                              | (0.00)  |
| $N$   | 88  | 86     | 111    | 111             | 111                                 | 111   |

$P$  = Probability that the correlation of  $r$  or greater would have arisen by chance ( $r$  values corresponding to  $P > 0.05$  are identified by an asterisk).

$N$  = Number of observations.

runs, 11 were discarded, because their computed values of  $u_*$  were too small ( $<0.025 \text{ m s}^{-1}$ ) to be very reliable. The remaining 140 runs were divided into the following stability categories based on the value of  $u_* = u_*/fL$ :

- Near neutral ( $\mu_* < 10$ ) —29 runs
- Moderately stable ( $10 \leq \mu_* \leq 50$ )—41 runs
- Very stable ( $50 < \mu_* \leq 100$ ) —44 runs
- Extremely stable ( $\mu_* > 100$ ) —26 runs

Of these, the near-neutral observations were used only for correlating  $h$  with  $u_*/f$ , since  $L$  and other diagnostic heights are not reliably determined under near-neutral conditions.

The sodar-measured values of  $h$  were correlated with the various diagnostic height parameters for different stability categories and their various combinations. The computed correlation coefficients together with a measure of their significance are given in Table 1. The corresponding coefficients of linear regression between  $h$  and diagnostic heights are given in Table 2 together with the standard errors of their estimates. Table 3 gives the same

for the regression line forced through the origin. The best-fitted linear regression lines are given as

$$\left. \begin{aligned} h &= mh_D + c \\ h &= nh_D \end{aligned} \right\}, \quad (15)$$

in which  $h_D$  may be any one of the observed and diagnostic heights. Obviously, the line with a finite intercept would be a better representation of the data than that with zero intercept, even though the latter might have a better theoretical and physical justification.

A number of inferences can be drawn from Tables 1–3. For moderately stable conditions,  $h_u$  has no significant correlation, while  $h_\theta$  has the best correlation ( $r \approx 0.53$ ) with  $h$ . For very stable runs, on the other hand,  $h$  is best correlated with  $h_u$  ( $r \approx 0.54$ ), while its correlations with  $h_\theta$ ,  $L$  and  $(Lu_*/f)^{1/2}$  are slightly lower but of comparable magnitudes ( $r \approx 0.4$ ). None of the diagnostic heights are significantly correlated with  $h$  under extremely stable conditions; the best correlation ( $r \approx 0.33$ ) is obtained with  $h_u$ . The correlation of  $h$  with  $L$ ,  $u_*/f$  or  $(Lu_*/f)^{1/2}$  improves considerably when moderately and very stable categories are combined, and even

TABLE 2. The coefficients ( $m$  and  $c$  values) of linear regression between the observed PBL height  $h$  and the diagnostic height parameters.

| Stability class   | Diagnostic height parameters |        |                 |                                     |   |
|---|------------------------------|--------|-----------------|-------------------------------------|---|
|   | $h_u$                        | $L$    | $\frac{u_*}{f}$ | $\left(\frac{Lu_*}{f}\right)^{1/2}$ | $\left(\frac{1}{30L} + \frac{f}{0.35u_*}\right)^{-1}$ |
| <b>Moderately stable</b><br>( $10 \leq \mu_* \leq 50$ ) |                              |        |                 |                                     |   |
| $m$   | -0.16                        | 0.78   | 0.058           | 0.25                                | 0.22  |
| ( $e_m$ )   | (0.39)                       | (0.28) | (0.029)         | (0.09)                              | (0.09)  |
| $c$   | 243.6                        | 177.1  | 126.4           | 145.9                               | 127.3   |
| ( $e_c$ )   | (61.8)                       | (19.8) | (50.4)          | (29.8)                              | (39.2)  |
| <b>Very stable</b><br>( $50 < \mu_* \leq 100$ )         |                              |        |                 |                                     |   |
| $m$   | 0.08                         | 3.31   | 0.048           | 0.43                                | 0.27  |
| ( $e_m$ )   | (0.21)                       | (1.14) | (0.025)         | (0.17)                              | (0.11)  |
| $c$   | 12.0                         | 108.9  | 108.9           | 106.0                               | 106.1   |
| ( $e_c$ )   | (38.6)                       | (17.1) | (24.4)          | (20.2)                              | (20.6)  |
| <b>Extremely stable</b><br>( $\mu_* > 100$ )            |                              |        |                 |                                     |   |
| $m$   | 0.39                         | 2.12   | 0.018           | 0.21                                | 0.13  |
| ( $e_m$ )   | (0.24)                       | (4.02) | (0.043)         | (0.41)                              | (0.25)  |
| $c$   | 51.9                         | 112.1  | 111.4           | 111.4                               | 111.2   |
| ( $e_c$ )   | (41.2)                       | (17.7) | (21.9)          | (19.5)                              | (19.0)  |
| <b>All stable cases with <math>\mu_* \geq 10</math></b> |                              |        |                 |                                     |   |
| $m$   | 0.18                         | 1.34   | 0.076           | 0.34                                | 0.27  |
| ( $e_m$ )   | (0.20)                       | (0.16) | (0.009)         | (0.036)                             | (0.028)   |
| $c$   | 133.2                        | 133.2  | 87.8            | 113.5                               | 105.4   |
| ( $e_c$ )   | (33.5)                       | (6.9)  | (11.2)          | (8.0)                               | (8.7)   |

$e_m$  = standard error of the estimate of  $m$ .  
 $e_c$  = standard error of the estimate of  $c$  in meters.



TABLE 3. The coefficients ( $n$  values) of linear regression with zero intercept between the observed PBL height  $h$  and the diagnostic height parameters.

| Stability class                                | Diagnostic height parameters |        |                 |                                     |   |
|--|------------------------------|--------|-----------------|-------------------------------------|---|
|  | $h_u$                        | $L$    | $\frac{u_*}{f}$ | $\left(\frac{Lu_*}{f}\right)^{1/2}$ | $\left(\frac{1}{30L} + \frac{f}{0.35u_*}\right)^{-1}$ |
| Moderately stable<br>( $10 \leq \mu \leq 50$ ) |                              |        |                 |                                     |   |
| $n$  | 1.32                         | 2.98   | 0.13            | 0.67                                | 0.50  |
| ( $e_n$ )                                      | (0.13)                       | (0.23) | (0.006)         | (0.037)                             | (0.024)   |
| Very stable<br>( $50 < \mu_* \leq 100$ )       |                              |        |                 |                                     |   |
| $n$  | 0.88                         | 9.88   | 0.15            | 1.25                                | 0.78  |
| ( $e_n$ )                                      | (0.04)                       | (0.68) | (0.009)         | (0.080)                             | (0.050)   |
| Extremely stable<br>( $\mu_* > 100$ )          |                              |        |                 |                                     |   |
| $n$  | 0.69                         | 24.4   | 0.22            | 2.33                                | 1.45  |
| ( $e_n$ )                                      | (0.05)                       | (3.13) | (0.024)         | (0.27)                              | (0.17)  |
| All stable cases with $\mu_* \geq 10$          |                              |        |                 |                                     |   |
| $n$  | 1.12                         |        | 0.14            | 0.74                                |   |
| ( $e_n$ )                                      | (0.063)                      |        | (0.004)         | (0.027)                             |   |

$e_n$  = Standard error of the estimate of  $n$ .

more so when all the stable runs with  $\mu_* > 10$  are considered together. On the contrary, its correlations with  $h_\theta$  and  $h_u$  drop to very low and insignificant values when all the cases are included in the analysis. On the whole, the best results ( $r \approx 0.67$ ) are obtained when  $h$  is correlated either with  $(Lu_*/f)^{1/2}$  or with Deardorff's interpolation formula. Since  $(Lu_*/f)^{1/2}$  also has the best theoretical support as a diagnostic height parameter, its use might be preferable to the other height parameters considered here.

Fig. 4 is a scatter diagram of  $h$  vs  $(Lu_*/f)^{1/2}$ , in which the data are separated according to our chosen stability categories. The best regression relation

considering all the data is

$$h = 113.5 + 0.34 \left(\frac{Lu_*}{f}\right)^{1/2}, \quad (16)$$

although, the theoretically better-supported relation

$$h = 0.74 \left(\frac{Lu_*}{f}\right)^{1/2} \quad (17)$$

may also be adequate for moderately stable conditions.

Because of the expected very high correlation between the values of  $u_*$  and  $L$  during nighttime at a land site, when the surface heat flux does not

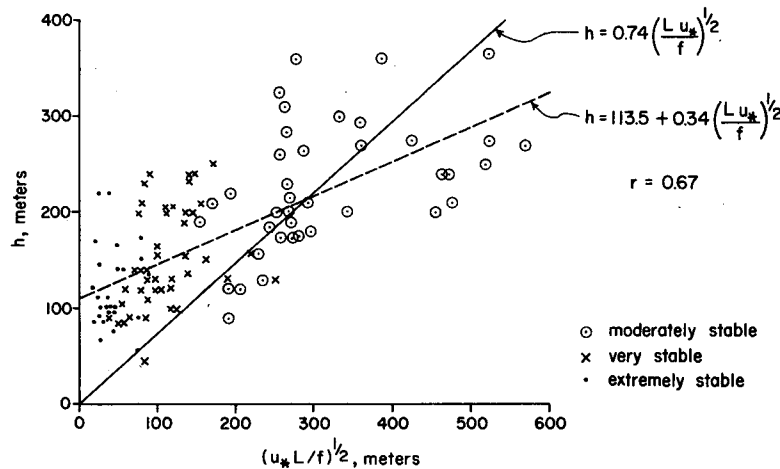


FIG. 4. Scatter diagram of  $h$  vs  $(Lu_*/f)^{1/2}$  for the various stability categories, and the best-fitted regression lines with and without the zero intercept.

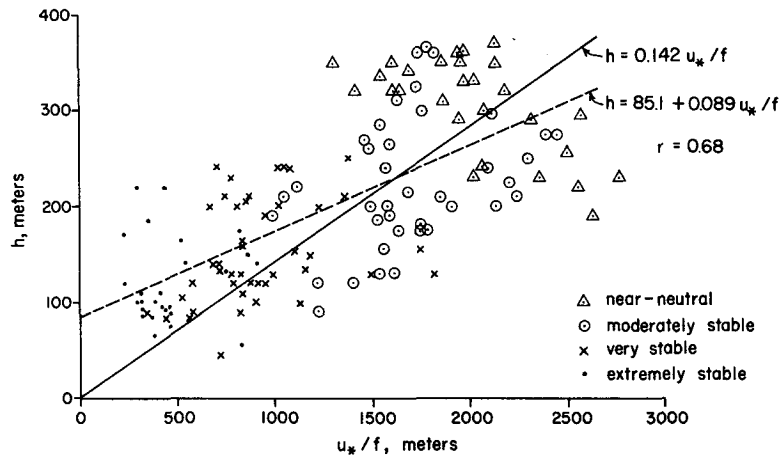


FIG. 5. Scatter diagram of  $h$  vs  $u_*f$  for the various stability categories and the best-fitted regression lines with and without the zero intercept.

vary over a wide range (Mahrt and Heald, 1979), it is not surprising to find that  $h$  is almost as well correlated with  $L$  and  $u_*f$  as it is with  $(Lu_*f)^{1/2}$ . Since the coefficients of linear regression with  $u_*f$  also show comparatively less variation with stability, it may be considered as a better predictor than  $L$  in parametric relations for  $h$ .  $u_*f$  is also much easier to determine as compared to  $L$  or  $(Lu_*f)^{1/2}$ . The scatter diagram of Fig. 5 shows as good a correlation between  $h$  and  $u_*f$  as found between  $h$  and  $(Lu_*f)^{1/2}$ , especially when the runs corresponding to the near-neutral stability category are also included in the correlation and regression analysis. The regression relation

$$h = 85.1 + 0.089 \frac{u_*}{f} \tag{18}$$

or

$$h = 0.142 \frac{u_*}{f}, \tag{19}$$

where  $h$  and  $u_*f$  are in meters, may be used as a diagnostic parametric relations for the mixed-layer height. While Eq. (18) gives a better representation of the extremely stable data, Eq. (19) may be expected to be a better representative of not only the near-neutral data shown in Fig. 5, but quite likely also of those which might fall farther away toward the neutral side, well beyond the range of the present data.

For the very stable and extremely stable categories, the height of the maximum in wind speed appears to be a good measure of  $h$  (however, note that the regression coefficient is  $<1$ ). For the extremely stable category, the Cabauw data indicates a minimum threshold value of  $\sim 50$  m and an average value of  $\sim 100$  m for the mixed-layer height during extremely stable conditions. Whether these figures would be representative of other more

homogeneous rural sites remains to be seen. It may be pointed out that the sodar measurements have an estimated error margin of 30 m and may not be relied upon for resolving the mixed layer height when  $h \leq 50$  m.

### 5. Conclusions and recommendations

A critical assessment is made here of the various diagnostic relations that have been proposed in the literature for the nocturnal boundary layer height. The parametric relations involving the wind and temperature profile characteristics of the whole boundary layer are less reliable and require more complicated observations than those involving only the surface layer variables. The latter are tested against the February 1975 experiments at Cabauw, the Netherlands, in which direct measurements of the mixed-layer height ( $h$ ) were made simultaneously with profile measurements on 20 and 213 m masts. Earlier tests of the same against the Great Plains and Wangara boundary layer observations (Hanna, 1969; Yu, 1978) were somewhat tentative and inconclusive due to the lack of direct measurement of  $h$ .

We have also suggested a new method of calculating  $u_*$  and  $L$  from observations of mean velocity and temperature at two levels one of which might fall outside the surface layer.

Having performed a correlation and regression analysis between  $h$  and the various other height parameters, we find that, considering all the data,  $h$  is best correlated ( $r \approx 0.67$ ) with  $(Lu_*f)^{1/2}$  and also equally well correlated with  $u_*f$ . The regression relations (16) and (18) may be considered as the best diagnostic relations. Equation (17) is found to be adequate only for moderately stable conditions, although it has been given by far the most theoretical

support. The simplest parameterization of  $h$  is provided by Eq. (19), which appears to be quite satisfactory for all but extremely stable ( $\mu_* > 100$ ) nighttime conditions. The correlations of  $h$  with  $u_* f$ ,  $(u_* L/f)^{1/2}$  and Deardorff's interpolation height are found to be much stronger ( $r \approx 0.67$ ) than those estimated by Yu (1978) using the Wangara data and  $h_i$  in place of  $h$ .

During conditions of strong stability ( $\mu_* > 50$ ), the height of the maximum in wind speed provides a good measure of  $h$ . The height of  $h_\theta$ , to which significant cooling extends, is found to be a comparatively poor measure of  $h$ .

*Acknowledgments.* The Cabauw data used here were provided to the author by Prof. Joost A. Businger and Dr. F. T. M. Nieuwstadt. The author would like to thank them for their many helpful comments and suggestions. This research was supported by the Atmospheric Research Section, National Science Foundation, through their Grant ATM77-21785.

#### REFERENCES

- Arya, S. P. S., 1975: Geostrophic drag and heat transfer relations for the atmospheric boundary layer. *Quart. J. Roy. Meteor. Soc.*, **101**, 147-161.
- , 1977: Suggested revisions to certain boundary layer parameterization schemes used in atmospheric circulation models. *Mon. Wea. Rev.*, **105**, 215-227.
- , and A. Sundararajan, 1976: An assessment of proposed similarity theories for the atmospheric boundary layer. *Bound.-Layer Meteor.*, **10**, 149-166.
- Benkley, C. W., and L. L. Schulman, 1979: Estimating hourly mixing depths from historical meteorological data. *J. Appl. Meteor.*, **18**, 772-780.
- Blackadar, A. K., 1957: Boundary layer wind maxima and their significance for the growth of nocturnal inversions. *Bull. Amer. Meteor. Soc.*, **38**, 283-290.
- Brost, R. A., and J. C. Wyngaard, 1978: a model study of the stably stratified planetary boundary layer. *J. Atmos. Sci.*, **35**, 1427-1440.
- Businger, J. A. and S. P. S. Arya, 1974: The height of the mixed layer in the stably stratified planetary boundary layer. *Advances in Geophysics*, Vol. 18A, Academic Press, 73-92.
- , J. C. Wyngaard, Y. Izumi and E. F. Bradley, 1971: Flux-profile relationships in the atmospheric surface layer. *J. Atmos. Sci.*, **28**, 181-189.
- Caughy, S. J., J. C. Wyngaard and J. C. Kaimal, 1979: Turbulence in the evolving stable boundary layer. *J. Atmos. Sci.*, **36**, 1041-1052.
- Deardorff, J. W., 1972a: Numerical investigation of neutral and unstable planetary boundary layers. *J. Atmos. Sci.*, **29**, 91-115.
- , 1972b: Parameterization of the planetary boundary layer for use in general circulation models. *Mon. Wea. Rev.*, **100**, 93-106.
- Hanna, S. R., 1969: The thickness of the planetary boundary layer. *Atmos. Environ.*, **3**, 519-536.
- Laikhtman, D. L., 1961: *Physics of the Boundary Layer of the Atmosphere*. GIMIZ, Leningrad, 200 pp. [NTIS OTS 64-1106].
- Lettau, H. H., and B. Davidson, Eds., 1957: *Exploring the Atmosphere's First Mile*, Vols. 1 and 2. Pergamon Press, 578 pp.
- Mahrt, L. J., and R. C. Heald, 1979: Comments on "Determining height of the nocturnal boundary layer." *Appl. Meteor.*, **36**, 383.
- , —, D. H. Lenschow, B. B. Stankov and I. Troen, 1979: An observational study of the structure of the nocturnal boundary layer. *Bound.-Layer Meteor.*, **17**, 247-264.
- Melgarejo, J. W., and J. W. Deardorff, 1974: Stability functions for the boundary layer resistance laws based upon observed boundary-layer heights. *J. Atmos. Sci.*, **31**, 1324-1333.
- Nieuwstadt, F. T. M., 1978: The computation of the friction velocity  $u_*$  and the temperature scale  $T_*$  from temperature and wind velocity profiles by least-squares methods. *Bound.-Layer Meteor.*, **14**, 235-246.
- , 1980: A rate equation for the inversion height in a nocturnal boundary layer. *J. Appl. Meteor.*, **9**, 1445-1447.
- , 1981: The steady state height and resistance laws of the nocturnal boundary layer: Theory compared with Cabauw observations. *Bound.-Layer Meteor.*, **20**, 3-17.
- , and A. G. M. Driedonks, 1979: The nocturnal boundary layer: A case study compared with model calculations. *J. Appl. Meteor.*, **16**, 115-129.
- , and H. Tennekes, 1981: A rate equation for the nocturnal boundary-layer height. *J. Atmos. Sci.*, **38**, 1418-1428.
- Pollard, R. T., P. B. Rhines and R. O. R. Y. Thompson, 1973: The deepening of the wind-mixed layer. *Geophys. Fluid Dyn.*, **3**, 381-404.
- Rao, K. S., and H. F. Snodgrass, 1979: Some parameterizations of the nocturnal boundary layer. *Bound.-Layer Meteor.*, **17**, 15-28.
- Rosby, C. G., and R. B. Montgomery, 1935: The layer of frictional influence of wind and ocean currents. *Pap. Phys. Oceanogr. Meteor.*, **3**, 101 pp.
- Smeda, M., 1979: Incorporation of planetary boundary-layer processes into numerical forecasting models. *Bound.-Layer Meteor.*, **16**, 115-129.
- Taylor, G. I., 1915: Eddy motion in the atmosphere. *Phil. Trans. Roy. Soc. London*, **A215**, 1-26.
- Wyngaard, J. C., 1975: Modeling the planetary boundary layer-extension to the stable case. *Bound.-Layer Meteor.*, **9**, 441-460.
- Yamada, T., 1979: Prediction of the nocturnal surface inversion height. *J. Appl. Meteor.*, **18**, 526-531.
- Yu, T., 1978: Determining height of the nocturnal boundary layer. *J. Appl. Meteor.*, **17**, 28-33.
- Zeman, O., 1979: Parameterization of the dynamics of stable boundary layers and nocturnal jets. *J. Atmos. Sci.*, **36**, 792-804.
- Zilitinkevich, S. S., 1972: On the determination of the height of the Ekman boundary layer. *Bound.-Layer Meteor.*, **3**, 141-145.
- , and J. W. Deardorff, 1974: Similarity theory for the planetary boundary layer of time-dependent height. *J. Atmos. Sci.*, **31**, 1449-1452.
- , and A. S. Monin, 1974: Similarity theory for the atmospheric boundary layer. *Izv. Atmos. Ocean. Phys.*, **10**, 587-599.